Efficient waveguide couplers using tilted gratings for optoelectronic interconnects

Jianhua Gan, Bipin Bihari, Linghui Wu, Feiming Li, Michael Dubinovsky and Ray T. Chen

Microelectronics Research Center
Department of Electrical and Computer Engineering
The University of Texas at Austin, Austin, TX 78758

Suning Tang

Radiant Research Inc., 9430 Research Blvd., Suite IV305, Austin, TX 78759

Abstract

Surface relief gratings with tilted grating profiles have been studied for efficient optical signal coupling for polymeric waveguide based optoelectronic interconnects. In this article the theoretical formulation used to calculate the diffraction efficiency in a pre-defined direction is discussed. The designed gratings provide an effective unidirectional surface-normal optical coupling for polymer-based optoelectronic interconnects. The gratings with a tilt-angle of 32 degrees and periods ranging from 0.5 to 3 μm were fabricated. Both surface-normal input and output grating couplers have been demonstrated in polyimide waveguides on silicon substrate.

Keyword: waveguide grating coupler, optical interconnect, MCM interconnect

Introduction

The electrical interconnects are facing their fundamental bottle-necks (such as speed, packaging, fanout, and power dissipation) with demand driven advancements in the high performance computing and data communication systems. Multichip module (MCM) technology is employed to provide higher clock speeds and circuit densities [1,2]. However, as cycle time and pulse widths generated by silicon VLSI circuit shrink, the bandwidth needed to preserve the rising and falling edges of the signals increases, the state-of-the-art technologies based on electrical interconnects fail to provide the required clock speed and communication distance in intra-MCM and inter-MCM hierarchies. Implementation of optoelectronic elements to provide high speed, large fanout interconnects is already a major thrust for many high performance systems where electrical interconnects failed to provide the bandwidth requirement. Employment of optoelectronic devices and components appears a necessity in high speed (200 MHz), wafer-scale interconnections. To make optical interconnects acceptable to microelectronics industry, it is pivotal to make the insertion of optics compatible with silicon CMOS fabrication process such that technology improvement and cost effectiveness are coupled together. Polymer-based optical waveguide technology, is particularly interesting for wafer-scale MCM interconnect applications for its high density and potentially low cost.

Effective optical coupling in the waveguide and out of the waveguide is one of the major problem in many optoelectronic interconnection schemes. In the applications where further device layers need to be integrated after the optoelectronic interconnection layer, the interconnection layer must be planar[3]. The second type of applications require the non-blocking communication among many modules[4]. Figures 1(a) and 1(b) illustrate two such applications. Currently, based on the state-of-the-art optical waveguide technology, insertion of optical interconnects for module-to-module connections is realized by using 45° total internal reflection mirrors in conjunction with vertical cavity surface emitting lasers (VCSELs) and

SPIE Vol. 3288 • 0277-786X/98/$10.00

high-speed photodetectors. Such a non-planarized coupling configuration is contradictory to the existing 3D electrical interconnects that are fabricated through microlithography [Fig. 1(a)]. The depth of the 45°

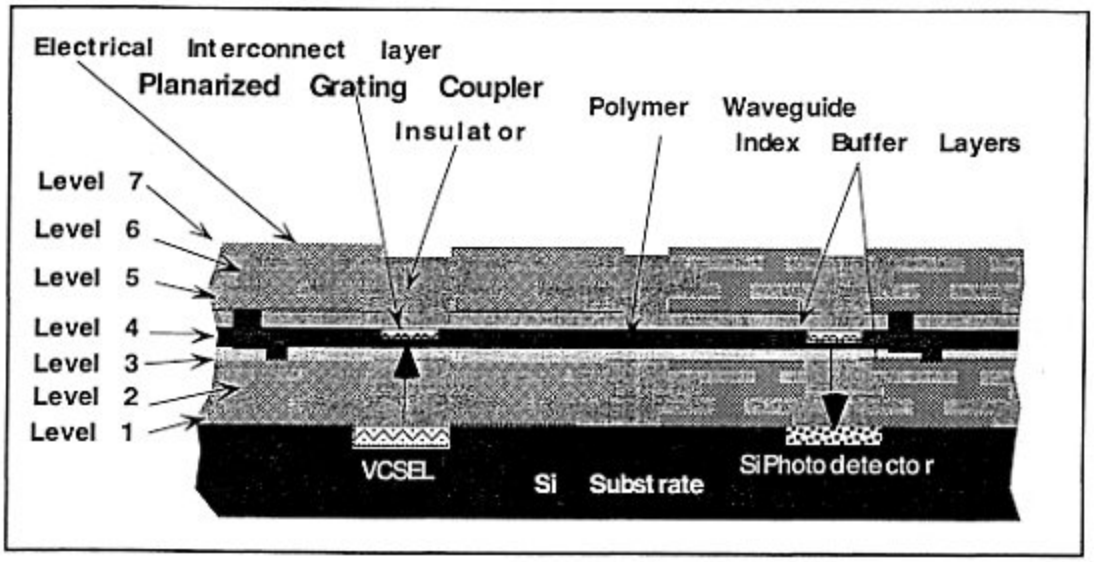

(a)

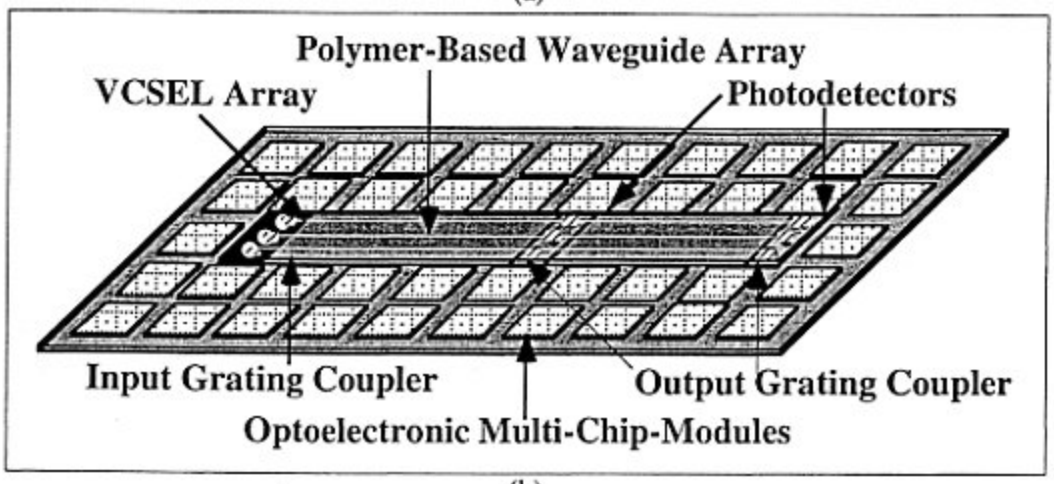

(b)

Fig.1. (a) Cross section of a optical vias for 3D optoelectronic interconnects. (b) Schematic of an optoelectronic interconnection link for wafer-scale MCMs using polymer-based waveguides.

mirror is typically in the order of 25 μm that is well-above the depth of focus of any submicron lithographic machines. As a result, no interconnection layer can be added over the optical waveguide layer with the non-planarized 45° mirror coupler. Further more, due to the transmission blocking nature of the 45° total internal reflection mirror, only point-to-point optical interconnection can be constructed. This severely limits its applications for high density MCM interconnections. On the other hand, planarized grating coupler can be designed with desired coupling efficiency in a specified direction, and is fully compatible with Si-CMOS processing.

Theoretical frame-work

The phenomenon of grating-coupled radiation is widely used in guided-wave optical interconnects. However, the surface-normal coupling scenario in optical waveguides has not been carefully investigated so far. Very often coupling in a specific direction is required. To achieve this unidirectional coupling the tilted grating profile can be used. Very important aspect of manufacturing of such couplers is the tolerance interval of the profile parameters, such as the tooth height, the width, the tilt-angle, etc. Gratings with very tight interval would be very difficult to manufacture and practically useless. Problems of gratings design were described in many publications[5-8]. However, described numerical methods works well only when grating profile is relatively shallow, and fail, when grating becomes deep. Thus, the new analytical methods, which provides high numerical accuracy were designed. Grating couplers with tilted profile demonstrate, as will be shown below, very high coupling efficiency in a given direction.

Formulation

Consider the grating structure shown in Fig. 2. For simplicity we derive equation for the TE mode, however, in the case of TM mode, the resulting equation is similar. A transverse electric (TE) mode guided E field is along the z-direction and satisfies:

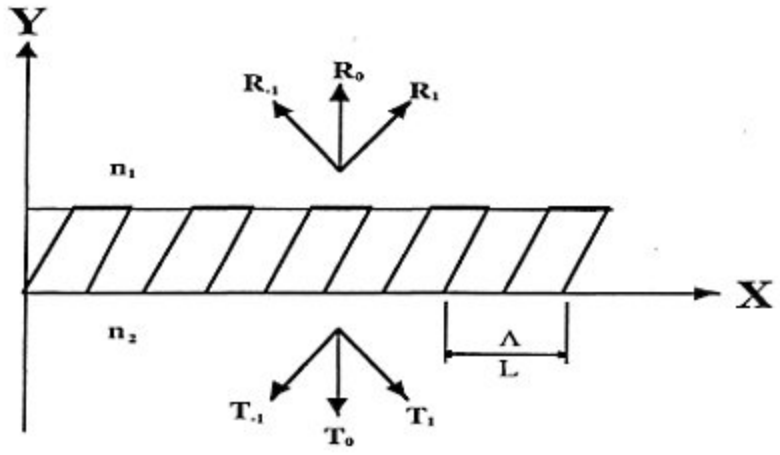

Fig. 2. The grating structure under consideration.

$$\frac{\partial^2 E_z}{\partial x^2}+\frac{\partial^2 E_z}{\partial y^2}+k^2(x,y)E_z=0 \qquad (1)$$

where a time dependence $\exp(-iwt)$ has been omitted, $k(x,y)$ is the wave vector with $k(x,y)=k_0 n(x,y)$, $k_0=2\pi/\lambda$, λ is the free space wavelength, $n(x,y)$ is the refractive index.

We can express field E_z as an Floquet's infinite summation of partial waves:

$$E_z(x,y)=\sum_{m=-\infty}^{\infty}E_m(y)\exp(i\alpha_m x) \qquad (2)$$

where: $\alpha_m=\alpha_0+m\frac{2\pi}{\Lambda}$ and Λ is the grating period, α_0 is a phase constant.

Outside groove region, in the area $y>h$, using Rayleigh expansion we can write:

$$E_{m1}(y) = \delta_m \exp(i\beta_1 y) + R_m \exp(i\beta_{m1} y) \quad (3)$$

where: $\beta_{m1} = \sqrt{k_1^2 - \alpha_{m1}^2}$, $\delta_m = 1$ when m=0 and $\delta_m = 0$, otherwise.

Below the groove region, in the area $y > 0$, the electric field can be written for each corresponding m as :

$$E_{m3}(y) = T_m \exp(-i\beta_{m2} y) \quad (4)$$

where:

$$\beta_{m2} = \sqrt{k_2^2 - \alpha_{m2}^2} \quad (4)$$

Inside groove region $0 < y < h$, $k^2(x,y)$ is periodic in the x direction and can be represented by a Fourier series of

$$k^2(x,y) = \sum_{m=-\infty}^{\infty} C_m(y) \exp(2\pi i m x / \Lambda) \quad (5)$$

Upon substituting (2) and (5) into equation (1) and collecting all terms with the same x-dependence, we can obtain equation at the region $0 < y < h$:

$$\frac{\partial^2 E_{m2}(y)}{\partial y^2} - \alpha_m^2 E_{m2}(y) + \sum_q C_{m-q}(y) E_{q2}(y) = 0 \quad (6)$$

Equation (6) can be written in a matrix form of

$$\mathbf{E_2''} = \mathbf{V(y)E_2} \quad (7)$$

where $\mathbf{E_2}$ is a column vector whose elements are E_{m2} and $\mathbf{V}(y)$ is a known square matrix whose elements are defined by:

$$V_{mn} = \begin{cases} \alpha_n^2 - C_0, & m = n \\ C_{n-m}, & m \neq n \end{cases} \quad (8)$$

The solution of (7) is subject to the boundary condition of E_z and $\partial E_z / \partial y$ being continuous at $y = h$ and $y = 0$. Taking the boundary conditions into account, we get:

$$\begin{cases} E_m'(0) + i\beta_{m2} E_m(0) = 0 \\ E_m'(h) - i\beta_{m1} E_m(h) = -2i\beta\delta_m exp(-i\beta h) \end{cases}$$

This can be written in matrix form as follows:

$$\begin{cases} \mathbf{E'(h)} + \mathbf{U_h E(h)} = \mathbf{S} \\ \mathbf{E'(0)} + \mathbf{U_0 E(0)} = \mathbf{0} \end{cases} \quad (9)$$

where $\mathbf{U_0}, \mathbf{U_h}$ are diagonal known matrices whose diagonal elements are:

$[U_0]_m = i\beta_{m2}$, $[U_h]_m = -i\beta_{m1}$

and $\mathbf{S}$ is a column matrix which in fact reduces to $[S]_m = -2i\beta \exp(-i\beta h)$, m=0.

Solution

In the case of rectangular profile Fourier coefficients in (5) are constants:

$$C_{Rm}(y) = {}^{i}\!/_{2\pi m}(k_2 - k_1)\left[\exp(-2\pi i m\, {}^{t}\!/_{\Lambda}) - 1\right] \qquad (10)$$

For the known height y, the tilted groove refraction index distribution can be considered as the rectangular groove distribution by making a shift along x direction as shown in Fig. 3: $d(y) = y\tan\varphi$, where φ is the tilt-angle.

According to the rules of Fourier-transformation, a coordinate shift in the original function creates a phase shift in the transformation result. Thus, the tilted profile coefficients can be written as:

$$C_m(y) = \exp(-2i\pi m y\tan(\varphi)/\Lambda)C_{Rm} = \exp(\gamma i m y)C_{Rm} \qquad (11)$$

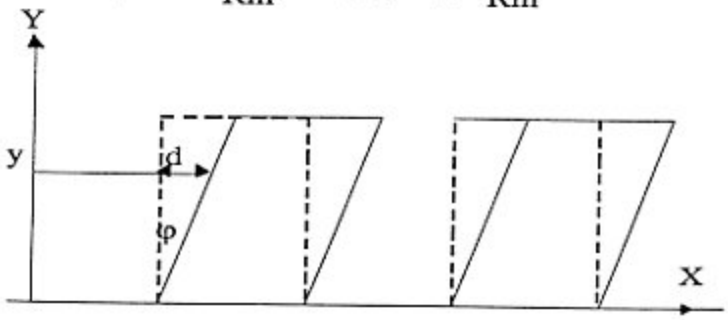

Fig. 3. Consideration of a tilted grating as a shifted rectangular grating.

Matrix $\mathbf{V}(y)$, in the case of tilted grating, can be written as follows:

$$\mathbf{V}(y) = \mathbf{Q}(y)\mathbf{V}_R\mathbf{Q}^*(y), \qquad (12)$$

where $\mathbf{Q}$ is diagonal matrix whose elements are: $[Q]_n = exp(\gamma i y n)$, $n = 1, 2, \ldots$, and the sign * means complex conjugation. Now, equation (7) can be rewritten as:

$$\mathbf{E}''(y) = \mathbf{Q}(y)\mathbf{V}_R\mathbf{Q}(y)\mathbf{E}(y) \qquad (13)$$

We can introduce a new matrix variable:

$$\mathbf{D}(y) = \mathbf{Q}(y)\mathbf{E}(y) \qquad (14)$$

Derivatives of the $\mathbf{Q}$ matrix can be found:

$$\mathbf{Q}'(y) = \mathbf{P}\mathbf{Q}(y), \quad \mathbf{Q}''(y) = \mathbf{P}^2\mathbf{Q}(y) \qquad (15)$$

where $\mathbf{P}$ is a constant diagonal matrix:

$$[P]_n = ni\gamma$$

From (13),(14) and (15) we can derive the equation:

$$\mathbf{D}'' + 2\mathbf{P}\mathbf{D}' + (\mathbf{P}^2 - \mathbf{V}_R)\mathbf{D} = 0 \qquad (16)$$

This equation is a second-order differential equation with constant coefficients and its general solution is:

$$\mathbf{D} = \exp(\mathbf{W}_1 y)\mathbf{A} + \exp(\mathbf{W}_2 y)\mathbf{B} \qquad (17)$$

Where **exp** is the exponential function from matrix (computation of this function will be discussed below), $\mathbf{A}$, $\mathbf{B}$ are constant matrices that are determined from boundary condition. In (17) matrix multiplication is non-commutative operation, so order of its fractions is important. $\mathbf{W}_1$, $\mathbf{W}_2$ matrices are roots of a second-order matrix equation:

$$\mathbf{W}^2 + 2\mathbf{PW} + (\mathbf{P}^2 - \mathbf{V}_R) = 0 \tag{18}$$

The boundary condition (9) can be written as:

$$\begin{cases} \mathbf{D}'(\mathbf{h}) + \left(\mathbf{U}_\mathbf{h} - \mathbf{P}\right)\mathbf{D}(\mathbf{h}) = \mathbf{Q}(\mathbf{h})\mathbf{S} \\ \mathbf{D}'(\mathbf{0}) + \left(\mathbf{U}_\mathbf{0} - \mathbf{P}\right)\mathbf{D}(\mathbf{0}) = \mathbf{0} \end{cases} \tag{19}$$

Using (17) and (19) we can find constant matrices $\mathbf{A}$, $\mathbf{B}$:

$$\begin{cases} \mathbf{A} = \left(\mathbf{W}_1 + \mathbf{U}_\mathbf{h} - \mathbf{P}\right)^{-1}\left(\mathbf{W}_2 + \mathbf{U}_\mathbf{h} - \mathbf{P}\right)\mathbf{B} \\ \mathbf{B} = \Big[\left(\mathbf{W}_2 + \mathbf{U}_\mathbf{h} - \mathbf{P}\right)\exp(\mathbf{W}_2\mathrm{h}) - \left(\mathbf{W}_1 + \mathbf{U}_\mathbf{h} - \mathbf{P}\right)\exp(\mathbf{W}_1\mathrm{h}) \\ \qquad \left(\mathbf{W}_1 + \mathbf{U}_\mathbf{h} - \mathbf{P}\right)^{-1}\left(\mathbf{W}_2 + \mathbf{U}_\mathbf{h} - \mathbf{P}\right)\Big]^{-1}\mathbf{Q}_\mathbf{h}\mathbf{S} \end{cases} \tag{20}$$

The above equations give exact analytical solution in the case of a tilted grating. In the case of rectangular grating, $\mathbf{W}_1$ and $\mathbf{W}_2$ matrices are $\mathbf{W}_1 = \mathbf{W}_2 = \mathbf{W}^{1/2}$

To calculate exponential function in (20) we can factorize $\mathbf{W}_1$ and $\mathbf{W}_2$ matrices:

$\mathbf{W}_\mathbf{m} = \mathbf{Z}_\mathbf{m}^{-1}\Omega_\mathbf{m}\mathbf{Z}_\mathbf{m}$ (m=1,2)

where $\Omega_\mathbf{m}$ is a diagonal matrix whose elements are the eigenvalues of $\mathbf{W}_\mathbf{m}$, and $\mathbf{Z}_\mathbf{m}$ is an orthogonal matrix whose columns are eigenvectors of $\mathbf{W}_\mathbf{m}$. Using exponential function series and matrix factorization we can write:

$$\exp(\mathbf{W}_\mathbf{m}\mathrm{h}) = \sum_{\mathrm{k}=0}^{\infty}\left(\mathbf{W}_\mathbf{m}\mathrm{h}\right)^\mathrm{k}/\mathrm{k!} = \sum_{\mathrm{k}=0}^{\infty}\left(\mathbf{Z}_\mathbf{m}^{-1}\mathbf{W}_\mathbf{m}\mathbf{Z}_\mathbf{m}\right)^\mathrm{k}\mathrm{h}^\mathrm{k}/\mathrm{k!} =$$

$$= \mathbf{Z}_\mathbf{m}^{-1}\left[\sum_{\mathrm{k}=0}^{\infty}\left(\mathrm{W}_\mathbf{m}\mathrm{h}\right)^\mathrm{k}/\mathrm{k!}\right]\mathbf{Z}_\mathbf{m} = \mathbf{Z}_\mathbf{m}^{-1}\exp(\mathbf{W}_\mathbf{m}\mathbf{h})\mathbf{Z}_\mathbf{m}$$

Thus, the exponential functions in (20) is: $\exp(\mathbf{W}_\mathbf{m}h) = \mathbf{Z}_\mathbf{m}^{-1}\hat{\Omega}_\mathbf{m}\mathbf{Z}_\mathbf{m}$, where $\hat{\Omega}_\mathbf{m}$ is a diagonal matrix whose elements are: $\left[\hat{\Omega}\right]_n = \exp(\Omega_n h)$. Coefficients R_n and T_n in (3), (4) can be found from condition of E_z being continuous at $y = h$ and $y = 0$. Energy in the n-th reflected and transmitted diffraction orders can be found:

$$E_R = R_n^* R_n \cos\alpha_{n1}$$
$$E_T = T_n^* T_n \cos\alpha_{n2} \qquad (21)$$

where * means complex conjugate.

To check the precision of numerical calculations, the energy balance can be used.

$$\sum_{n1} E_R + \sum_{n2} E_T = 1 \ .$$

Numerical Results.

The numerical results, presented below, are obtained utilizing equation (20), (21). The diffraction grating period is selected to make the angle of the first diffraction order α_1 equal to a defined value (for example, bouncing angle of a waveguide) and cut all other higher diffraction orders. In reflected light, only zero-order diffraction exists for this grating. The diffraction grating has a period equals to 0.9 of the wavelength value. Substrate refraction index is 1.45. Tooth width is selected to be one-half of the grating period. Fig. 4 is a plot of coupling efficiency in different diffraction orders versus tooth height (in μm) for the case of a rectangular grating profile. The coupling efficiency in this case is low.

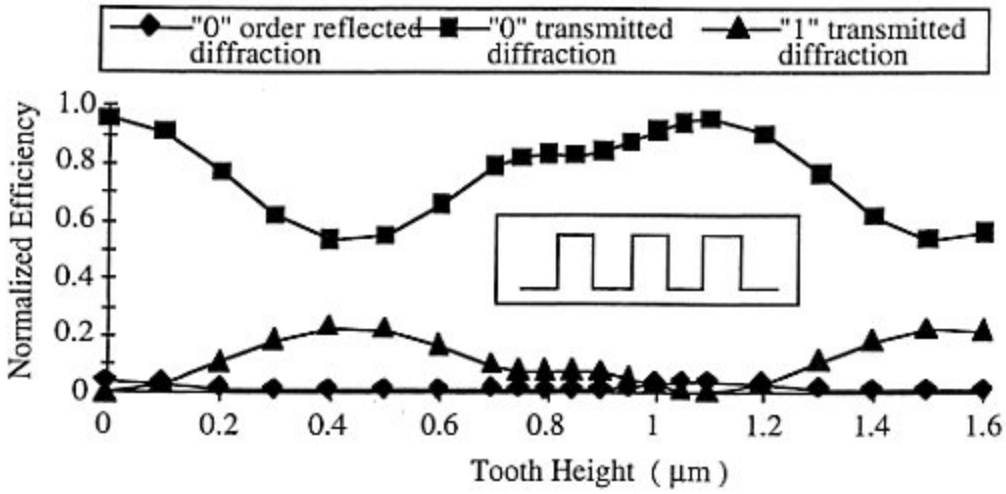

Fig. 4. Plot of coupling efficiency versus tooth height for a rectangular grating profile.

Fig.5 is a plot of coupling efficiency in different diffraction orders versus tooth height (in μm) for the case of a tilted grating profile. The tilt-angle of 32° was defined to obtain maximum coupling efficiency in the first diffraction order for a pre-defined first-order diffraction angle. This plot shows high coupling efficiency in the first diffraction order. In Fig. 6 we plot coupling efficiency versus tooth tilt-angle for the optimal tooth height of 1.1 μm. Fig. 7 is a plot of coupling efficiency versus tooth width. The tooth width is changing from 0 to 0.9 μm, which is the grating period value. Values of tooth tilt-angle and tooth height are kept equal to the optimum values. When tooth width equals zero or period value, only zero-order reflection and refraction radiation exist. When tooth width is between 0.4 μm and 0.6 μm, coupling efficiency into the first diffraction order is very high. This value diapason allows one to make the grating with a relatively large tooth width tolerance interval. In above case, allowable error equals to

0.1/0.5=20%, which is very good. Using the estimated optimum parameters we fabricated a number of grating structures and demonstrated the surface-normal coupling in the polyimide waveguide.

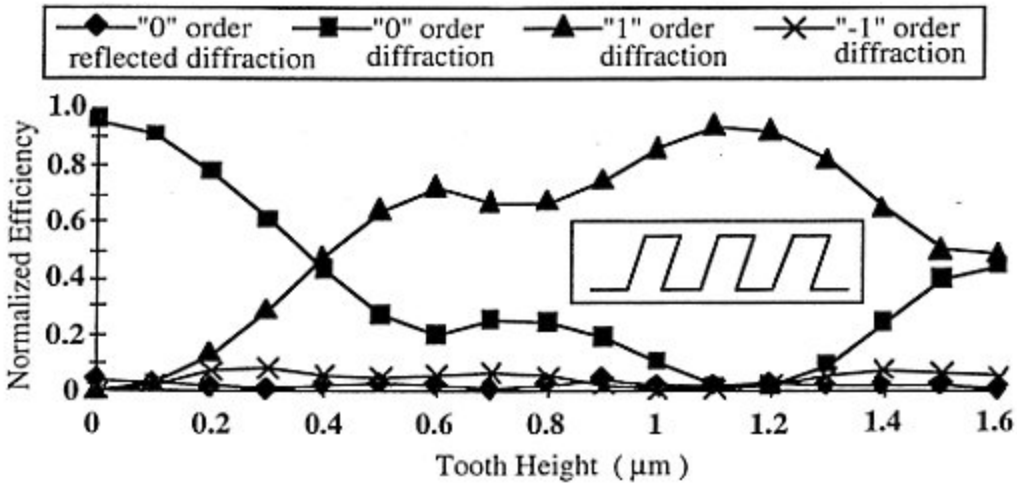

Fig. 5. Plot of coupling efficiency versus tooth height for a tilted grating.

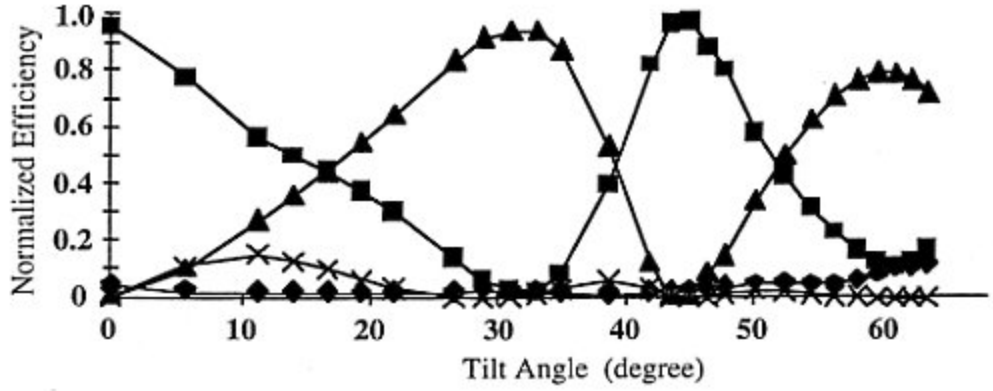

Fig. 6. Plot of coupling efficiency vs grating tilt angle for the optimal tooth height of 1.1 μm.

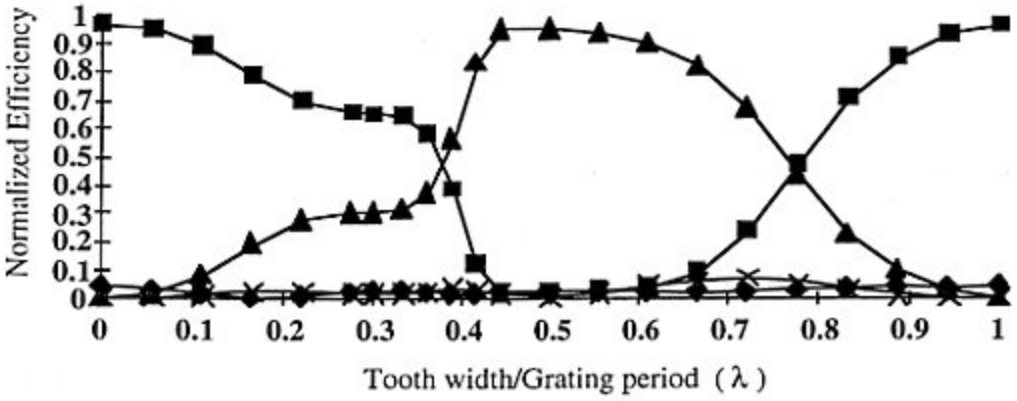

Fig. 7. Plot of coupling efficiency versus tooth width.

Fabrication of tilted gratings

The polyimide waveguide was first fabricated on silicon or quartz substrate by spin-coating. For silicon substrate, an A600 primer layer was spin-coated first on the substrate with a spin speed of 5000 rpm, and pre-baked at 90 ^{0}C for 60 seconds. The Amoco polyimide 9020D cladding layer was then spin-coated on Si substrate, followed by a 9120D core layer. A final curing at 260 ^{0}C in nitrogen atmosphere was carried out for more than three hours. Typical thickness of the waveguide was 7 μm. It should be noted that the polyimide waveguides can be fabricated on any substrate of interest including glass and quartz.

In order to fabricate the grating coupler by reactive-ion-etching (RIE), a thin aluminum metal mask was deposited on top of the polyimide-based planar waveguide. First, a 500-Angstrom aluminum layer was coated on top of the waveguide by electron beam evaporation deposition, followed by a layer of 5206E photoresist with spin speed of 3000 rpm. The grating pattern on photoresist was recorded by interfering two beam of the λ=442 nm He-Cd laser line. In order to record a grating with a period of Λ, the cross angle θ of the two interference beams is determined through the formula of $\sin(\theta/2) = \left(\lambda/2n\Lambda\right)$. After developing the grating pattern on photoresist, a post-bake at 120^{0}C for 30 minutes was followed. To transfer the photoresist grating patterns to aluminum, we used RIE to etch the aluminum in the opening window of the photoresist pattern. The gases used were $BCl_3/SiCl_4$ with a pressure of 20 millitorr. However, it was found that there were still some photoresist residuals in the grating groove which could block the aluminum RIE process. In order to clean these residuals, an additional step of RIE etching using oxygen was applied before removing the Al layer. To form the tilted grating pattern on the polyimide waveguide, we used a RIE process with a low oxygen pressure of 10 millitorr to transfer the grating pattern on aluminum layer to the polyimide layer. In order to get the tilted profile, a Faraday cage [9] was used. The sample inside the cage was placed at a tilted angle of 32 degrees with respect to the incoming oxygen ions. Finally, the Al mask was removed by another step of RIE process.

Experimental results

Fig.8 shows a scanning electron microscope (SEM) picture of the microstructure of the tilted grating. The grating period can be tuned from 0.6 μm to 4 μm by changing the recording angles of the two-beam laser interference method. The schematic of coupling a surface-normal input light into and out of the waveguide using the device fabricated is shown in Fig.9(a), together with an experimental photograph in Fig.9(b). In Fig.9(b), the grating was designed to surface-normally couple the laser beam from free space

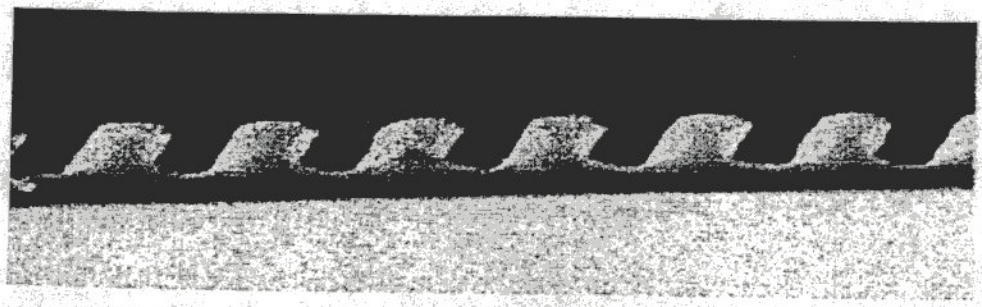

Fig. 8. SEM picture of the tilted grating.

into the waveguide with an operating wavelength at 1.3 μm, and from the waveguide back to free-space using a period grating coupler with the period as that of the input grating but oppositely tilted. The coupling into the planar waveguide with the unidirectional propagation can be clearly observed with a

measured throughput efficiency of 5-10%. The coupling efficiency is relatively low because the difference between the refractive index of the guiding and cladding layers of the waveguide is very small (~0.015). Our calculations indicates that the coupling efficiency could be significantly improved by increasing the refractive index difference and optimizing the microstructure of the grating. We also found that the output coupling efficiency close to 100% can be achieved simply by increasing the interaction length associated with the output grating. For the grating of about 3 mm we measured an efficiency of 35-40%. If multiple output grating couplers are employed along the waveguide and the grating parameters (i.e. depth, length, etc.) are adjusted such that the coupling efficiencies of the output gratings increase along the waveguide propagation direction, the uniform multi-stage optoelectronic interconnect can be realized among the modules. Further experiments such as increasing Δn are underway to improve the coupling efficiency of the surface-normal gratings.

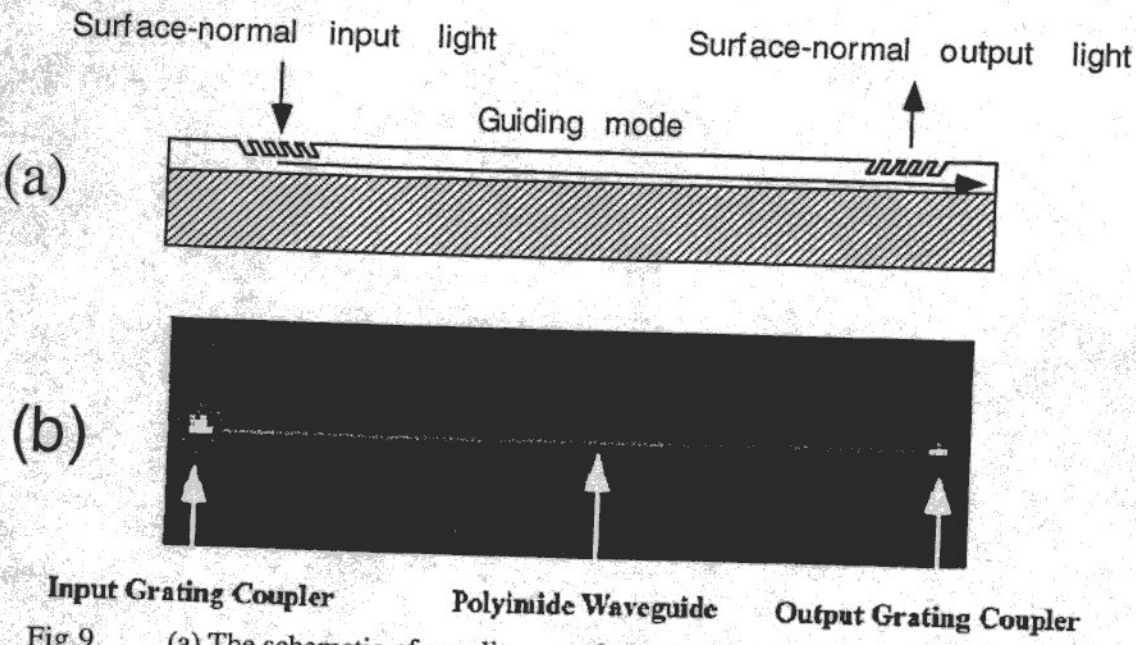

Fig.9 (a) The schematic of coupling a surface-normal input light into waveguide and coupling out from the waveguide using the tilted grating. (b) The experimental photograph of polyimide waveguide with tilted grating showing coupling-in and coupling-out 1.3 μm light.

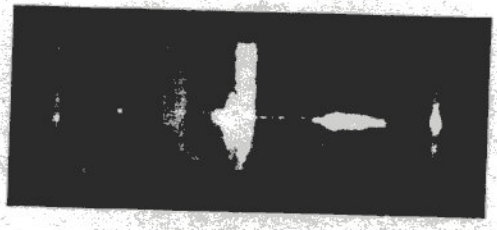

Fig.10 Photograph of surface normal output coupling

Conclusion

In conclusion, we have designed and fabricated the tilted grating for unidirectional surface-normal waveguide grating couplers for polyimide waveguides. The gratings with a tilt-angle of 32 degrees and periods ranging from 0.5 to 3 μm were fabricated. Both surface-normal input and output grating couplers have been demonstrated in polyimide waveguides on silicon substrate. The throughput efficiencies of 5-

10% have been achieved in these gratings. Further experiments such as increasing Δn and grating depths are underway to improve the coupling efficiency of the surface-normal gratings.

References

[1] D.P.Seraphim and D.E.Barr, "Interconnect and packaging technology in the 90's", Proc. SPIE 1390, pp.39-54, 1990.

[2] C.Neugerbauer, R.O.Carlson, R.A.Fillion, and T.R.Haller, "Multichip module designs for high performance applications", in Multichip Modules, Compendium of 1989 Papers, pp.149-163, International Electronic Packaging Society, 1989.

[3] K.S.Giboney, "Parallel-optical Interconnect Development at HP Laboratories", Proc. SPIE, Optoelectronic Interconnects and Packaging IV, Editor: Ray Chen and P. Guilfoyle, Vol.3005, pp.193-201, 1997.

[4] Y.Liu, J.Bristow, K.Jhonson, A.Peczalski, T.Marta, S.Bounnak, W.Goldberg, and B.Hanzal, "Polymer optical waveguide technology for multichip modules (MCMs) and board level interconnects", Proc. SPIE, Vol.2891, pp. 88-95, 1996.

[5] Toshiaki Suhara and Hiroshi Nishihara, "Integrated optics components and devices using periodic structures", IEEE J. of Quantum Electronics, Vol. QE-22, no. 6, pp. 845-867, 1996.

[6] D.Brundrett, E.Glystis, and T.Gaylord, "Homogeneous layer models for high-spatial-frequency dielectric surface-relief gratings", Appl. Opt. Vol. 33, no. 13, pp. 2695-2760, 1994.

[7] M. Li and S.J.Sheard, "Waveguide couplers using parallelogramic-shaped blazed gratings", Opt. Comm., Vol. 109, pp. 239-245, 1994.

[8] T. Tamir and S. T. Peng, "Analysis and design of grating couplers", Appl. Phys., Vol. 14, pp. 235-254, 1977

[9] G.D.Boyd, L.A.Coldren, F.G.Storz, "Directional reactive ion etching at oblique angles", Appl. Phys. Lett., Vol. 36, no. 7, pp. 583-585, 1980. 1. D.P.Seraphim and D.E.Barr, "Interconnect and packaging technology in the 90's", Proc. SPIE 1390, pp.39-54, 1990.